
Coherent Lidar Turbulence Measurement for Gust Load Alleviation

David Soreide, Rodney K. Bogue, L.J. Ehernberger, and
Hal Bagley

August 1996



National Aeronautics and
Space Administration

Coherent Lidar Turbulence Measurement for Gust Load Alleviation

David Soreide
Technical Consultant
Seattle, Washington

Rodney K. Bogue and L.J. Ehernberger
NASA Dryden Flight Research Center
Edwards, California

Hal Bagley
Coherent Technologies, Inc.
Boulder, Colorado

1996



National Aeronautics and
Space Administration

Dryden Flight Research Center
Edwards, California 93523-0273

Coherent lidar turbulence measurement for gust load alleviation

David Soreide

Technical Consultant
Seattle, Washington 98105

Rodney K. Bogue and L.J. Ehernberger

NASA Dryden Flight Research Center
Edwards, California 93523-0273

Hal Bagley

Coherent Technologies, Inc.
Boulder, Colorado 80306

ABSTRACT

Atmospheric turbulence adversely affects operation of commercial and military aircraft and is a design constraint. The airplane structure must be designed to survive the loads imposed by turbulence. Reducing these loads allows the airplane structure to be lighter, a substantial advantage for a commercial airplane. Gust alleviation systems based on accelerometers mounted in the airplane can reduce the maximum gust loads by a small fraction. These systems still represent an economic advantage. The ability to reduce the gust load increases tremendously if the turbulent gust can be measured before the airplane encounters it. A lidar system can make measurements of turbulent gusts ahead of the airplane, and the NASA Airborne Coherent Lidar for Advanced In-Flight Measurements (ACLAIM) program is developing such a lidar. The ACLAIM program is intended to develop a prototype lidar system for use in feasibility testing of gust load alleviation systems and other airborne lidar applications, to define applications of lidar with the potential for improving airplane performance, and to determine the feasibility and benefits of these applications. This paper gives an overview of the ACLAIM program, describes the lidar architecture for a gust alleviation system, and describes the prototype ACLAIM lidar system.

1. INTRODUCTION

This paper describes the alleviation of gust loads as a new application for an airborne lidar system. The basic system architecture, preliminary modeling results, performance requirements, and preliminary specifications of a lidar system which can be used for proof-of-concept studies of a gust load alleviation system are presented. This work is being done under the NASA Airborne Coherent Lidar for Advanced In-Flight Measurements (ACLAIM) program.

The underlying principle of the pulsed lidar measurement of variations in windspeed (turbulence) is the doppler shift in the frequency of laser-emitted light energy that is scattered from atmospheric aerosols. Selection of the range of the lidar beam along the atmospheric path for inquiry is based on the timing of receiver actuation (range-gating). The laser pulses are transmitted into the atmosphere forward of the aircraft and scattered off naturally occurring particles (aerosols) entrained in the ambient flow field. Operation of the lidar is affected by pulse energy, pulse length, distance of measurement, and atmospheric backscatter coefficient (β). The backscatter coefficient is defined as the ratio of backscattered energy to the incident radiant energy normalized by distance and solid angle of emission.

The ACLAIM program is based on a radical change in the way airborne lidar is expected to be used. In the past, lidar systems were seen in the context of airborne radar because these systems provided a hazard warning to the pilot.¹ By viewing the lidar as an integral part of the airplane control system, warning lead time requirements can be substantially reduced, and the utility can be dramatically extended.

To see this distinction, consider a single example, the detection of clear air turbulence. To provide a 30-sec pilot warning (a typical requirement), the lidar must have a maximum range of more than 7 km.¹ The desired precision and update rates at this range stretches or exceeds the capabilities of airborne lidar systems, particularly if the backscatter coefficient is low. If, on

the other hand, the lidar signal were incorporated into the control system, the control surfaces could be automatically moved to reduce the impact of the turbulence. In most conditions, substantial reductions can be made in the effect of a gust with a lidar range of only a few hundred meters² This reduction is felt to be achievable with a near-term, state-of-the-art lidar system.

The concept of incorporating the lidar signal into the control system is described by the term “feed-forward.” The correcting signal is derived from a source forward in time from the controlled parameter and is fed forward into the summing junction. This concept differs from a conventional system where this signal is from a delayed source and is fed “back” to the control system summing junction.

1.1 Other lidar technology applications

The benefits of the ACLAIM program, while not limited to a single aircraft, have focused primarily on the High-Speed Civil Transport (HSCT). For this airplane, two major areas can benefit from the feed-forward lidar system. The first is gust load alleviation. The second application is the prevention of unstarts in the supersonic inlet. The approach is to detect the presence of a turbulent patch of air before the airplane enters it and automatically increase the inlet unstart margins. These margins are maintained in this condition until the lidar measurements show that the turbulent conditions have subsided. At this time, the margins are reduced for more efficient operation. The distance of measurement for the inlet unstart application is substantially larger (on the order of 1 km) than that for gust load alleviation.

1.2 Development approach

The ACLAIM program was divided into three tasks. The first, and larger, effort is to develop a prototype lidar system. In the short term, this task will provide data on lidar performance. The second task is to define the lidar operating environment. As perceived by the ACLAIM program, the two most important factors in the environment are the natural aerosol populations without which the concept cannot function and the atmospheric turbulence which is the subject of the measurement. The third task is to define an architecture for an installed airplane control system incorporating the lidar. From the results of the second and third tasks, the requirements on the lidar and on the airplane control system and the expected benefits can be estimated. In follow-on studies, not currently funded, the ACLAIM test bed lidar is expected to be used in prototypes of integrated airplane control systems.

As a consequence of the broad spectrum of technical skills required, the ACLAIM team includes representatives from several organizations. The team involved in the ACLAIM program is composed of personnel from NASA Dryden Flight Research Center, Edwards, California, Coherent Technologies, Inc., Boulder, Colorado, (Lidar Development), and Institute for Global Change Research and Education, IGCRE, Huntsville, Alabama, (Atmospheric Aerosol Science). Other NASA centers and two universities are contributing to this effort. Potential beneficiaries of lidar development, such as The Boeing Company, Seattle, Washington, U.S. Navy, and U.S. Air Force, are providing technical experts which serve on the technical steering committee. In addition, The Boeing Company is exploring feed-forward gust alleviation for the HSCT using internal research and development funds, and a collaboration has been established to investigate the prevention of inlet unstarts and gust alleviation. Table 1 lists ACLAIM program participants.

Table 1. ACLAIM program organization.

Participant	Role
Air Force-Wright Laboratories	Technical steering committee
Alabama A&M University	Atmospheric turbulence modeling
Boeing-Seattle	Inlet unstart requirements Gust load alleviation requirements Technical steering committee
Coherent Technologies, Inc.	LIDAR sensor developer

Table 1. Concluded.

Participant	Role
David Soreide	Technical consultant
IGCRE-University of Alabama/Huntsville	Tropospheric aerosol modeling
NASA-Ames	DC-8 flight operation
NASA-Dryden Flight Research Center	NASA lead center Project management Project engineering SR-71 flight operation
NASA-Langley Research Center	Technical steering committee Laser science Flight systems Atmospheric science (stratosphere)
NASA-Marshall Space Flight Center	Technical steering committee Laser technology
NASA-Lewis	Technical steering committee Propulsion controls requirements Inlet requirements
U.S. Navy-Warminster	Technical steering committee Military requirements
North Carolina A&T University	Gust load alleviation control systems studies

Intended results of the ACLAIM project include developing a prototype lidar system for use in feasibility testing of gust load alleviation systems and in testing other airborne lidar applications, defining applications of lidar with potential for improving airplane performance, and determining the feasibility and benefits of these applications. The evaluation of the benefit and feasibility of the ACLAIM prototype lidar with respect to speed, altitude, and atmospheric properties will be performed in flight testing on the NASA DC-8 and SR-71 aircraft.

2. NOMENCLATURE

ACLAIM	Airborne Coherent Lidar for Advanced In-Flight Measurements
c	speed of light
CW	continuous wave
$D(s)$	atmospheric structure function
E	lidar pulse energy, mJ
ECU	environmental control unit
erf	error function
f	optical system f -number
h	Planck's constant
HSCT	High-Speed Civil Transport
IF	intermediate frequency
IGCRE	Institute for Global Change Research and Education, Huntsville, Alabama

L_o	turbulence outer scale, m
LO	local oscillator
MO	master oscillator
MSU	mass storage unit
n	lidar pulse rate, pulses/sec
P/CEU	power/control electronics unit
$P(v)$	probability that lidar measurement error exceeds velocity (v)
$P(v, \sigma(\beta) \beta)$	probability of measurement error exceeds velocity, given $\sigma(\beta)$
$p(\beta)$	probability density distribution of backscatter coefficient
R	range, m
s	distance between measurement points, m
s'	position in space, m
SNR	signal-to-noise ratio
SO	slave oscillator
SPU	signal processing unit
TRS	transmit/receive switch
v	velocity, m/sec
V_{radial}	radial, along the lidar beam axis, component of air velocity, m/sec
V_x	axial component of air velocity, m/sec
V_z	vertical component of air velocity, m/sec
V_1, V_2	radial component of air velocity for lidar beams 1 and 2
$V(s)$	scalar velocity field of atmospheric turbulence, m/sec
x	axial position, m
z	vertical position, m
β	atmospheric backscatter coefficient at $\lambda = 2\mu\text{m}$
η	system efficiency
θ	angle between lidar beams
λ	wavelength, m
ξ	system sample parameter, constant = 0.25
σ	standard deviation
σ_{atm}	standard deviation of atmospheric gust velocity
σ_g	geometric standard deviation
σ_{radial}	standard deviation of radial velocity measurement
σ_{total}	standard deviation of velocity measurement
σ_x	standard deviation of x component of velocity
σ_z	standard deviation of z component of velocity
σ_1, σ_2	standard deviation of radial component of individual lidar beams

3. GUST LOAD ALLEVIATION SYSTEM

3.1 Existing gust load alleviation background

Reduction of gust loads on a commercial airplane is not a new idea. The concept was used, for example, on an L-1011 (Lockheed, Palmdale, California) in 1980.² This application used accelerometers to monitor the movement of the wingtips, and the outboard ailerons were used to reduce the structural loads on the wing. The requirements of the system are relatively modest and are not considered flight critical.

The L-1011 load alleviation system reduces the gust loads at the wingtips, mainly to allow an increased aspect ratio wing. Recent work has been done to reduce the vertical acceleration at the airplane center of gravity.³ In this work, a test airplane was fitted with a gust measurement system mounted on a boom in front of the airplane. The gust measurements were passed to the control system, which operated the wing flaps and elevators, so the lift was controlled without pitching the airplane. With this limitation, reductions in the gust loads of as much as 90 percent in the center of the frequency band were achieved. Controlling the airplane using the elevators alone or controlling the axial accelerations using the engine thrust requires increasing the lead time because the airplane pitch rate and the engine thrust have slower response times. A lidar system can provide this lead time.

Gust alleviation using a lidar has been simulated⁴ using a Boeing 747 aircraft. Only the elevators were used to relieve the gust loads. To reduce the normal acceleration by 90 percent (equivalent to the study in reference 3), the lidar must measure vertical velocity 100 m in front of the airplane. Using a lidar, this requirement is reasonable. Comparing references 3 and 4 indicates that the distance ahead of the airplane that the sensor must gather information is determined by the actuator and aircraft response times.

3.2 Forward-looking sensor

If a lidar system is used to measure the gust velocities at some distance in front of the airplane, then the limitation of the actuator rates can be reduced. With sufficient lead time, feed forward gust alleviation system operation can be achieved with arbitrarily slow response at the expense of requiring longer range lidar measurements. The architecture of the gust alleviation system is being developed, and its description is outside the scope of this paper. This system is expected to function as a feed-forward controller so that it will have minimal design impact on the inner-loop flight control system. With these limitations, preliminary design studies²⁻⁴ indicate that the gust loads may be reduced by as much as 90 percent. In practice, this will be diminished because of gust measurement uncertainty and actuator rate limits. Preliminary estimates of these effects indicate that a 50 percent reduction in gust loads provides a substantial advantage for the airplane structure.

4. LIDAR SYSTEM REQUIREMENTS

4.1 Gust alleviation requirements summary

To achieve the benefits described in section 3, an objective of the ACLAIM design and flight test program is to develop lidar system requirements for active use in gust alleviation systems. Flight control for gust alleviation depends primarily on estimation of the vertical gust component encountered by the airplane. In some respects, this estimation increases the lidar sensor requirements for load alleviation beyond simply a warning that atmospheric turbulence intensity is increasing. Such warnings can be based on the lidar radial component alone and aimed forward along the flightpath. These warnings can be highly effective for supersonic inlet control by increasing the operating margin. At greater detection ranges, such warnings could also assist in accurately advising passengers to use seat belts. In this section, lidar measurement noise is described for selected examples of the sensing range from the airplane. Two example lidar installation configurations are used to discuss lidar accuracy considerations for gust alleviation. A simple estimate of the rate at which the measurement error would exceed an acceptable limit during a maximum gust encounter is also given.

Vertical gust velocity induces changes in the angle of attack which are much more effective at increasing gust loads than are changes in the axial gust velocity. Definition of the "look-ahead distance" is a subject of ongoing study, but a range on the order of 100–300 m is a reasonable estimate. The measurement error should be less than 25 percent of the gusts peak magnitude in order to maintain more than 50 percent of the optimum load reduction.*

*Private communication on 11/29/95 with V.M. Walton of Boeing Commercial Airplane Company.

4.2 Vertical velocity measurement

The measurement of the vertical velocity by an airborne lidar system has proven to be a difficult problem. Because a lidar system measures only the radial velocity component, the vertical velocity must be calculated from some set of radial velocity measurements. In the simplest case (fig. 1), radial velocity measurements are made at a given range and angle ($\theta/2$) above and below the flightpath. Then the velocity measured along the lidar beam, the radial velocity, is

$$V_{radial} = V_x \cos\left(\frac{\theta}{2}\right) - V_z \sin\left(\frac{\theta}{2}\right) \quad (1)$$

Where V_z is the z , or vertical component of the air velocity, and V_x is the x or axial component and θ is the angle between the two lidar beams. If two measurements are made above and below the flightpath, V_1 and V_2 , then these simultaneous equations can be solved for V_z .

$$V_z = \frac{V_1 - V_2}{2 \sin\left(\frac{\theta}{2}\right)} \quad (2)$$

If the standard deviation of V_1 and V_2 measurement noise components are equal to σ_{radial} , then the standard deviation of V_z is

$$\sigma_z = \frac{\sigma_{radial}}{\sqrt{2} \sin\left(\frac{\theta}{2}\right)} \quad (3)$$

This result for a simple case remains a lower noise limit for the more complex scan patterns that may be considered. The accuracy of the vertical velocity component can be improved by increasing the angle θ . The uncertainty is generally a function of the angles at which the measurement is made and is proportional to the standard deviation of the radial velocity measurement. Thus, accuracy of lidar used as a gust alleviation sensor depends on the installed configuration and on the inherent signal-to-noise (SNR) characteristics of the lidar system.

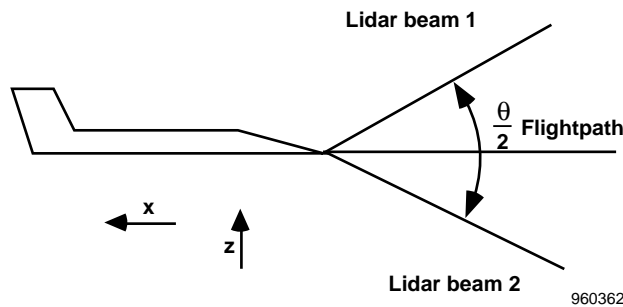


Fig. 1. Simplest case, configuration for lidar measurement of vertical velocity.

4.3 Atmospheric turbulence

The interpretation of lidar measurements is further complicated because atmospheric gust velocity varies in time and space. For estimation of the vertical gust component using the configuration illustrated in figure 1, the lidar radial velocity measurements are not made in the same place, and neither measurement is on the flightpath. To characterize the variations of gust

velocity with distance separating the lidar measurement regions, meteorological descriptions of atmospheric turbulence use the structure function for stationary turbulence.^{†,5} The structure function depends only on the spatial separation as shown in equation 4.

$$D(s) = \left\langle \left(V(s') - V(s' + s) \right)^2 \right\rangle \quad (4)$$

The brackets denote that $D(s)$ is an ensemble average quantity obtained by integration over all space within the stationary turbulence process, $V(s)$ is a scalar velocity field, s' is a position, and s is the scalar distance between s' and $s' + s$. If $s = 0$, then it is physically obvious that $D(s) = 0$. Atmospheric turbulence is often characterized by the Kolomogorov spectrum (with $-5/3$ slope[†]) with an outer scale (L_o) that represents the largest length of statistically probable correlation. For large separation distances, such as where $s > L_o$, the gust velocity correlations become essentially zero, then $D(s) \sim 2\sigma_{atm}^2$, two times the variance of the atmospheric gust velocity.⁵ At intermediate separation distances on the order of 300 m, the structure function can usually be estimated by

$$D(s) = 2\sigma_{atm}^2 \left(\frac{s}{L_o} \right)^{2/3} \quad (5)$$

If $D(s)$ is interpreted as the variance because of the separation s , then the measured vertical velocity standard deviation may be approximated as

$$\sigma_{total} = \sqrt{\sigma_z^2 + D(z)} \quad (6)$$

Where σ_{total} is the combined standard deviation of the vertical velocity, and z is the distance between the lidar measurement regions above and below the flightpath. Equation 6 shows that the accuracy of the measurement is affected by tradeoffs between measurement noise and the separation distances between lidar target regions (in turbulence). As the angle θ is increased, the uncertainty decreases (eq. 3), but the contribution of turbulence increases (eq. 5). In the limit where σ_z is small by virtue of larger viewing angles and noiseless lidar,

$$\sigma_{total} \approx \sqrt{2}\sigma_{atm} \left(\frac{z}{L_o} \right)^{1/3} \quad (7)$$

If L_o is 3000 m, and z is 300 m; then,

$$\sigma_{total} \approx 0.66 \sigma_{atm} \quad (8)$$

This contribution to the standard deviation resulting from gust variations between the separated lidar sensing regions above and below the flightpath, will dominate for measurements in turbulence where the system is used. This result indicates that spatial variation in the gust velocity at the two separated lidar-sensing regions would frequently prevent an acceptable level of performance for a viable gust load alleviation system. Therefore, the approach described in section 4.4 is assessed to explore a more effective configuration than the one shown in figure 1.

4.4 Proposed lidar configuration

To eliminate the contribution of the turbulence to the measurement error, mounting two lidar systems, one on the underside of the nose and the other at the top of the horizontal tail, is proposed. For HSCT, this mounting would separate the two systems by 13 m and, given a beam intersect location of 200 m in front of the airplane nose (fig. 2), yields an angle of 0.043 rad (2.5°). Because beam 2 is ideally along the flightpath, the angle between lidar beams is the angle between beam 1 and the flightpath as

[†]Tank, W.G., *Atmospheric Disturbance Environment Definition*, NASA Contractor Report CR-195315 (1994). [This report is not publicly available.]

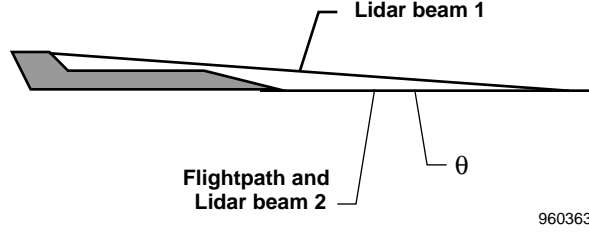


Fig. 2. Measurement geometry.

well as the angle between the two laser beams. Zero angle of attack is assumed, so for nonzero angle of attack, the angle between lidar beams will decrease to keep the sensed region on the flightpath.

The two lidars are aimed at the same spot 100 to 300 m in front of the airplane. Each lidar makes independent measurements of the radial velocity. These measurements are then combined to calculate the axial and vertical velocities. The advantage of this approach is that the measurement is on the flightpath; however, the angle between the measurements is small, increasing the uncertainty. These measurements may be made at short range, which improves the signal-to-noise ratio. Because the signal-to-noise ratio can be quite high, even for relatively low β , the resulting uncertainty in the vertical velocity is better than the approach proposed in figure 1. This approach also allows focusing of the lidar beam to limit the size of the measurement region, thus improving the spatial resolution.

The vertical velocity is

$$V_z = \left(\frac{V_1}{\sin(\theta)} - \frac{V_2}{\tan(\theta)} \right) \quad (9)$$

Where θ is the angle between the two beams and V_1 and V_2 are the two radial velocity measurements. Because the V_1 and V_2 radial component measurements are collocated, the turbulence structure function contribution becomes negligible, and the standard deviation of the vertical velocity is then given by

$$\sigma_z = \sqrt{\left(\frac{\sigma_1}{\sin(\theta)} \right)^2 + \left(\frac{\sigma_2}{\tan(\theta)} \right)^2} \quad (10)$$

Where σ_1 and σ_2 are the standard deviations of the radial velocity measurements.

4.5 Predicted performance

Using equation 10, the standard deviation of the velocity measurement may be calculated as a function of the backscatter coefficient. The standard deviation of the radial velocity measurements is given by reference 6.

$$\sigma_{radial}^2 = \frac{1}{32\sqrt{\pi}} \left(\frac{\lambda}{2} \right)^2 \frac{1}{n} \left(1 + \frac{8\sqrt{\pi}}{\text{SNR}} + \frac{\sqrt{\pi}}{3\xi^3 \text{SNR}^2} \right) \quad (11)$$

where λ is the laser wavelength, n is the number of pulses per second, $\xi = 0.25$, and the signal-to-noise ratio (SNR) is given by reference 7.

$$\text{SNR} = \frac{\eta E \beta \lambda^2}{2hc} \left(\frac{\pi}{2} + \tan^{-1} \left(\frac{\pi R}{4\lambda f^2} \right) \right) \quad (12)$$

where η is the system efficiency, E is the laser energy, β is the backscatter coefficient ($/\text{m}\cdot\text{sr}$), h is Planck's constant, c is the speed of light, R is the range, and f is the optical system f -number. Equation 12 uses the signal to noise ratio relationship for a continuous wave lidar system because the focal region is much shorter than the pulse length. With equations 10–12, σ_z values for the prototype ACLAIM lidar and a more powerful postulated follow-on system anticipated at the end of phase one of ACLAIM are calculated for 1-sec averages using 100 and 200 pulses/sec. Table 2 lists parameters for the prototype and follow-on systems.

Table 2. ACLAIM lidar and postulated lidar characteristics.

Parameter	Laser system comparison	
	ACLAIM lidar	Postulated lidar
System efficiency, η	0.08	0.08
Wavelength, μ	2.022	2.022
Pulse energy, mJ	25	125
Pulses per second	100	200
f -number	1000, 2000, 3000	1000, 2000, 3000
Pulse duration, μ sec	0.45	1.2

Figure 3 shows the result of substituting equations 11 and 12 into equation 10 with the values from table 2.

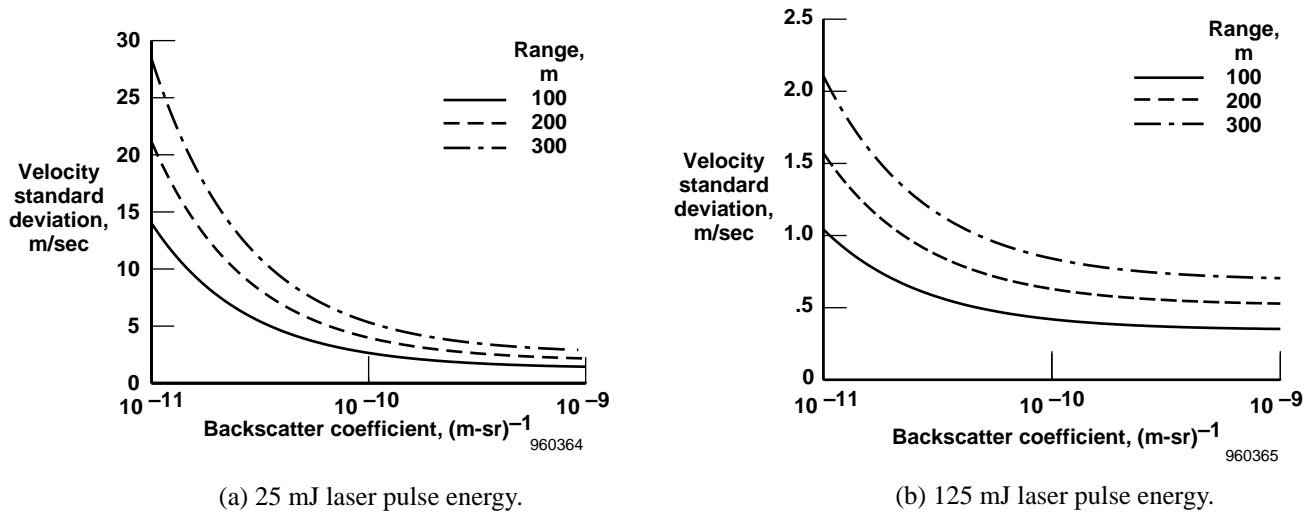


Fig. 3. Standard deviation of the velocity measurement as a function of the backscatter coefficient.

Figure 3 shows that the standard deviation of the measurement increases steeply at the low backscatter coefficients and that the standard deviations for the 125-mJ system are significantly improved. Note the ordinate range differences between figures 3(a) and 3(b). To interpret these results for a gust alleviation system, it is proposed to calculate the probability that the error on a velocity measurement will exceed a given tolerance level. Once the variation in the normal acceleration is known as a function of the error in the sensor measurement, this result can be interpreted as the probability that the gust alleviation system will fail to reduce the gust loads below a given level.

The probability that the measurement error will exceed a given value, v , for a fixed backscatter coefficient if the velocities are normally distributed is

$$P(v, \sigma_z, (\beta)|\beta) = 1 - \operatorname{erf}\left(\frac{v}{\sigma_z(\beta)\sqrt{2}}\right) \quad (13)$$

Where erf is the error function. If the probability density distribution function of β is known, the probability that the error will exceed v is

$$P(v) = \int_0^{\infty} P(v, \sigma_z, (\beta)|\beta) \frac{p(\beta)}{\beta} d\beta \quad (14)$$

Where $p(\beta)$, the probability density distribution of β , is a log-normal distribution. The log normal distribution $p(\beta)^\ddagger$ is shown in equation 15 and figure 4.

$$p(\beta) = \frac{1}{\ln(\sigma_g)\sqrt{2\pi}} e^{\left(\frac{-\left(\ln\left(\frac{\beta}{\beta_0}\right)\right)^2}{2(\ln(\sigma_g))^2}\right)} \quad (15)$$

Where β_0 , the geometric mean of the backscatter coefficient, is 3×10^{-10} /(m-sr) and σ_g is the geometric standard deviation ($\sigma_g = 2$). The viability of the 25-mJ system is indicated by observing that the velocity standard deviation at a 100 m range is projected to be on the order of 2 m/sec or less for backscatter coefficients of 3×10^{-10} or more, which are expected for the majority of flight test experience. Error implications with respect to extremely low backscatter values which may be expected over an airframe lifetime are discussed in section 4.6 with emphasis on the 125-mJ system performance.

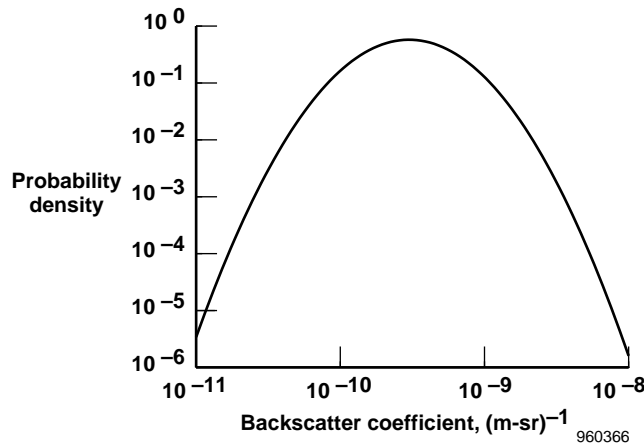
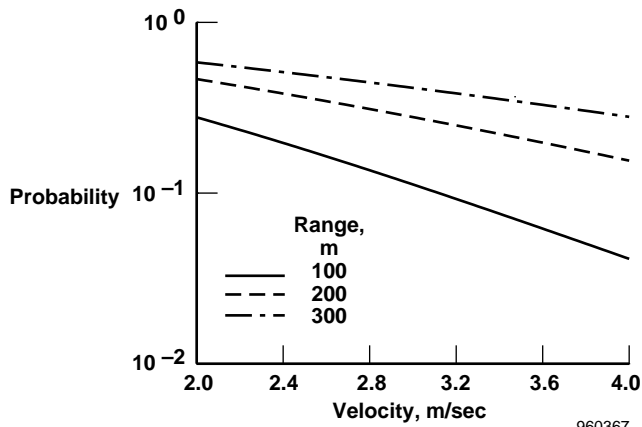


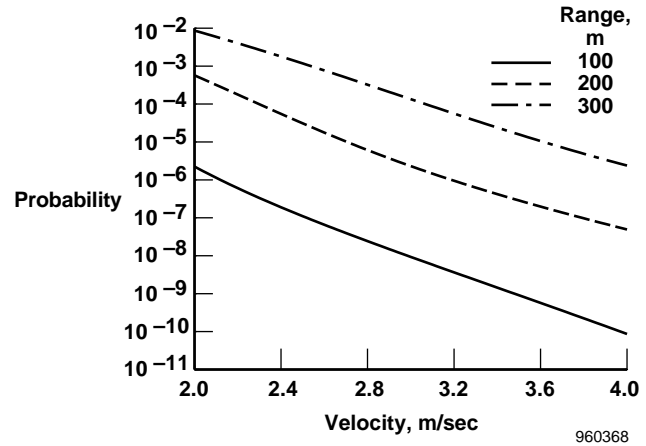
Fig. 4. The probability density distribution of β , the backscatter coefficient.

Using equation 14, the probability of a measurement exceeding a value v is plotted in figure 5(a) for the ACLAIM lidar and in figure 5(b) for the proposed lidar system. This is the fraction of the time that the error exceeds v . The rate at which this error

[‡]Private communication on 11/29/95 with David A. Bowdle of IGCRC.



(a) 25 mJ laser pulse energy.



(b) 125 mJ laser pulse energy.

Fig. 5. The probability that the velocity error exceeds v versus v in m/sec.

is exceeded is critically dependent on the spatial variation of the aerosol density, which is unknown. The great contrast between the probability of error for these two systems is obvious.

The Boeing Company has studied the variation in the ability of the control system to reduce the normal acceleration at the airplane center of gravity as the forward path gain of the control system is varied. For discrete, “1-cosine” shaped gusts as well as continuous random turbulence with the NASA Dryden spectral form, the reduction in the normal acceleration is greatly diminished if the feed-forward gain is changed from its optimum value by more than 25 percent. Changes in the feed-forward gain can be interpreted as being equivalent to the relative error in the gust velocity measurement. Reducing the gain by 25 percent has the same effect on the control system as making a gust velocity estimate that is 25 percent lower than the correct value. Therefore, if the relative error in the gust velocity measurement is larger than 25 percent, the effectiveness of the gust alleviation system is substantially reduced. In the performance estimates, 25 percent will be used as the maximum permissible relative error in the lidar measurement of gust velocity.

The magnitude of the maximum gust for which the alleviation system is designed is still being determined. For example, choose a gust magnitude of 16 m/sec (which has an exceedance rate of approximately 10^{-5} /hr). If the maximum error is 25 percent, then 25 percent of 16 m/sec = 4 m/sec. At 300 m range, the probability that the lidar error will exceed 4 m/sec is 2×10^{-6} . To calculate an error rate, the spectrum of the aerosol density variation must be known. If these variations were uniform and lasted 1-min each, then the error rate would be approximately 60 times the probability of error, or approximately 10^{-4} /hr. Combining this with the rate at which the gust exceeds 16 m/sec (approximately $\sim 10^{-5}$ /hr), the combined probability can be calculated that a 16 m/sec gust will be encountered and that the measurement error will exceed 4 m/sec, approximately 10^{-9} /hr. This rate is on the order of the requirement for a flight critical system.

4.6 ACLAIM lidar performance

In section 4.5, a lidar system which has significantly more pulse energy than the prototype lidar system being developed by ACLAIM has been postulated. As in many development programs, improvements in laser technology are expected to provide the additional power. The remaining question is whether the ACLAIM lidar can be used in prototypes of the gust alleviation system. The answer is yes. The requirement for increased laser power is driven by the self-imposed requirement that the lidar system have a rate at which the error exceeds 4 m/sec which is on the order of 10^{-4} /hr.

For more moderate values of the backscatter coefficient, the lidar performance is not as strong a function of the laser pulse energy. Figure 6 is a comparison between the performance of 125- and 25-mJ lidar systems at a range of 100 m. The standard deviation of the ACLAIM lidar at the center of the probability distribution of the backscatter coefficient (approximately 3×10^{-10} /(m-sr)) is 1.8 m/sec. This result is comparable to the standard deviation for the 125-mJ system near the lowest

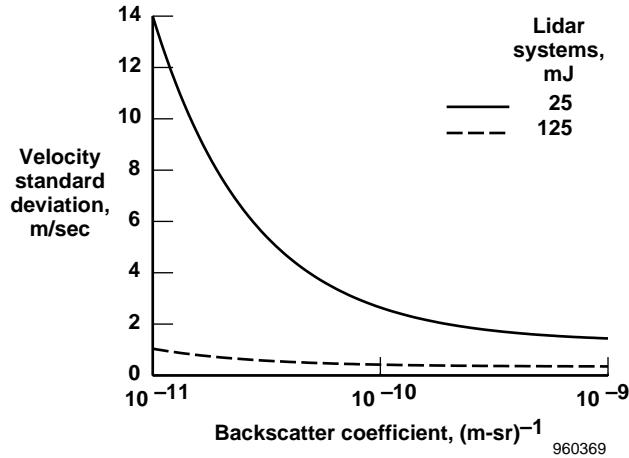


Fig. 6. Comparison between a 25- and 125-mJ lidar system at 100 m range.

backscatter coefficients. Clearly, the differences become much larger at extremely low backscatter conditions. Because the flight program is confined to a few tens of hours, encountering these extremely low backscatter conditions is unlikely.

5. ACLAIM LIDAR SYSTEM

5.1 System overview

The ACLAIM lidar system is a self-contained, modular configuration composed of five modules: optical transceiver, power/control electronics unit (P/CEU), signal processing unit (SPU), mass storage unit (MSU), and environmental control unit (ECU). The system architecture of figure 7 illustrates the functional operation of the coherent lidar system. The core of this system is a compact and highly efficient coherent laser radar transceiver based around a high-pulse-energy, diode-pumped, solid-state, 2- μm laser.

5.2 Optical transceiver

Figure 7 shows a block diagram of the transceiver. The heart of the lidar system is shown in the cross-hatched regions. The key subsystems and their functions are listed in table 3.

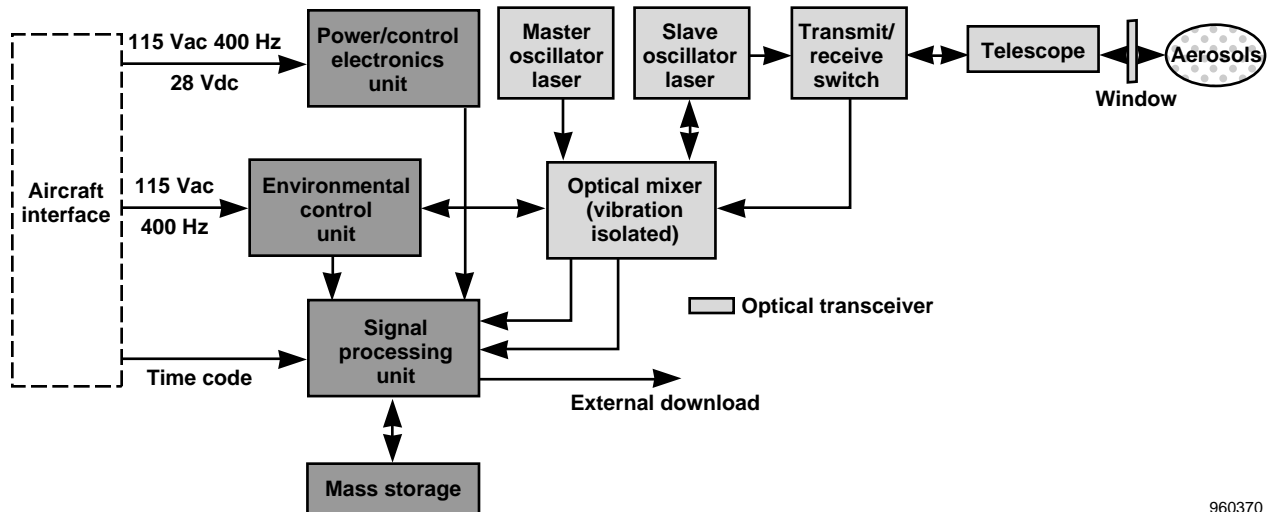


Fig. 7. Function block diagram.

Table 3. Key transceiver subsystems.

Subsystem	Function
Master oscillator (MO)	CW laser providing stable reference frequency used to injection-seed the SO and to act as the reference local oscillator (LO) in the coherent receiver.
Slave oscillator (SO)	Injection-seeded Q-switched laser providing high-energy laser pulses.
Transmit/receive switch (TRS)	Separates transmitted beam from received beam by imposing separate polarization states on the beams.
Telescope	Collimates outgoing SO beam and receives backscattered energy for mixing with local oscillator.
Optical mixing	Optical assembly used to route, split, and combine low-power optical signals.

As the name implies, the transceiver has two basic functions: produce and transmit high energy pulses and receive energy backscattered from atmospheric aerosols. In producing these pulses, a high degree of frequency stability is required because the transmitted pulses serve as a reference against which the received energy frequency is compared. The receiving process gathers the backscattered energy and mixes it with a small sample of the master oscillator energy to form a coherent detector. Coherent detection is used to improve the signal-to-noise ratio in the detection process.

The ACLAIM program provides a special challenge in that the high-speed operation of the HCST or the SR-71 airplane (Lockheed-Martin Corporation, Burbank, California) causes a particularly large doppler shift that is beyond the direct detection bandwidth of state-of-the-art detectors. Therefore, offsetting the mixing frequency in the coherent detection process to produce an in-band frequency which can then be detected is necessary. An acousto-optic modulator is used to accomplish this offset, termed the intermediate frequency or (IF) from the slave oscillator. A single telescope (a mono-static system) provides spatial optical gain to aim the beam in directions of interest and collects returning scattered energy. Once collected, this scattered energy is combined with light from the slave oscillator on the surface of a photodetector. The resultant IF photocurrent contains a heterodyne term consisting of the difference frequency between the intermediate frequency and the slave oscillator, thereby allowing the doppler frequency shift to be calculated and aerosol velocities to be determined by the signal processor. A master oscillator and a slave oscillator are the basis of the transceiver operation. The master oscillator produces low-power, frequency stable, continuous wave radiation at 2.022 nm. The slave oscillator produces the high-energy pulses and is forced to oscillate at the frequency of the master oscillator by an injected beam from the master oscillator. The slave oscillator is a pulsed, Q-switched laser pumped by several diode-lasers. This oscillator produces a pulse of radiation with an energy of 25 mJ at a repetition rate of 100 pulses/sec.

Based upon flight experiment objectives, previous transceiver development experience, laboratory demonstrations, and risk reduction efforts, the transceiver performance specifications were developed. Table 4 lists these specifications.

Table 4. Transceiver specifications.

Parameter	Value
Wavelength, nm	2.022
Laser pulse energy, mJ	25
Laser pulse duration, nsec	450
Laser line quality	$<1.3 \times$ transform limit
Pulse repetition rate, pulses/sec	100

Table 4. Concluded.

Parameter	Value
Telescope clear aperture, cm	10
Gaussian referenced beam quality	≤ 1.25
Beam pointing stability	≤ 10 percent far-field divergence
Heterodyne frequency stability	± 12 MHz @ 1σ
System efficiency (far field), percent	> 10
Size, ft ³	11
Weight, lb	400 (250 chiller)
Power, kW	3.6

5.3 Signal processor

The signal processor derives the turbulence information from the energy backscattered from the atmospheric aerosols. Signal processing includes a high-speed digitizer for the signal from the coherent detector; a real-time digital signal processor to transform the output information into the frequency domain; a master central processing unit to control the system operation; and cockpit, aircraft, and transceiver interfaces. Except for the analog front end, these components are commercially available. The semicustom design analog module will provide the desired dynamic range and linearity over the range of input frequencies. The self-contained system is responsible for measurements, data acquisition, and data storage.

5.4 Transceiver support hardware

The power/control electronics unit (P/CEU) controls the master and slave laser oscillators and monitors health and safety during operation. Because it records the data from the flight tests, the mass storage unit is critical to the success of the flight experiments. Environmentally rugged, reliable devices with high storage capacity are required to accommodate the large amount of data generated during an extended flight mission. A rugged hard disk drive will be used for this application.

The environmental conditioning unit provides cooling control to keep the transceiver and its submodules within 0.5 °C of 15 °C over the -28 °F to 55 °C temperature range of the internal airplane environment. The heat exchanger currently under consideration, comprising the bulk of the system size weight and power, occupies 6.4 ft³, weighs 250 lb, and produces 1 kW of cooling capacity.

Figure 8 illustrates these modules installed in the SR-71 airplane. The chiller and transceiver are installed in an outboard pylon mounted on the rear lower aircraft surface. The remainder of the system (SPU, P/CEU and MSU) is installed in an SR-71 compartment adjacent to the pylon.

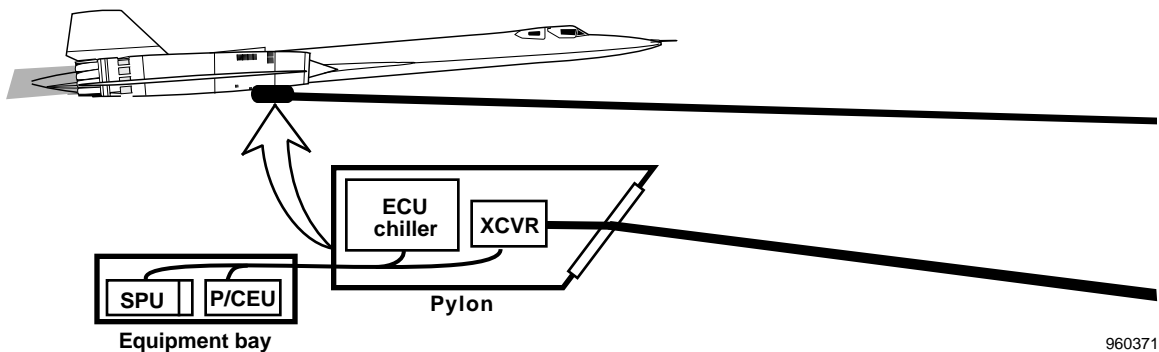


Fig. 8. The lidar system modules and mounting location in the SR-71.

6. FLIGHT TEST PLANS

The lidar system will be tested on NASA DC-8 and SR-71 test bed aircraft, and a preliminary analysis will be completed to show the feasibility of a lidar system for gust alleviation and inlet unstart prevention. This technology is being considered for the HSCT airplane, and the ACLAIM program hopes to answer the critical questions to decide whether or not to include lidar as part of the airplane control system. This work will provide prototype sensor technology needed for flight testing feed-forward gust alleviation and inlet unstart warning systems. The flight testing will be used to confirm the system feasibility and performance under nominal expected aerosol backscatter conditions. The outcome of the program is expected to be a set of studies of the costs and benefits of such a system and a prototype lidar system which is intended to subsequently be incorporated into feasibility test for gust alleviation and inlet unstart prevention.

7. CONCLUDING REMARKS

This paper describes work within NASA's Airborne Coherent Lidar for Advanced In-Flight Measurements (ACLAIM) program to explore the feasibility of a lidar-based gust alleviation system. Gust alleviation can be profitably applied to the High Speed Civil Transport and to subsonic airplanes. The paper reviews previous work and compares two methods for using a lidar as the gust sensor. Calculations show that a gust alleviation system incorporating a lidar as the gust sensor is feasible given reasonable improvements in the laser power. The ACLAIM lidar is described in detail and the planned flight testing of this system is discussed.

8. REFERENCES

1. Targ, R., "Airborne Lidar," *Airborne Wind Shear Detection and Warning Systems, Third Combined Manufacturers' and Technologists' Conference*, Hampton, Virginia, Oct. 16–18, 1991, pp. 2552–2570.
2. Bendixen, G.E., R.F. O'Connell, and C.D. Siegert, "Digital Active Control System for Load Alleviation for the Lockheed L-1011," *Aeronautical Journal*, Nov. 1981, pp. 656–663.
3. Hahn, K.U. and R. Konig, "ATTAS Flight Test and Simulation Results of the Advanced Gust Management System LARS," AIAA 92-4343, Aug. 1992.
4. Robinson, P.A., "The Use of Predictive Lidar Measurements in Alleviating Turbulence Induced Disturbances of Aircraft in Flight," *Tenth Annual International AeroSense Symposium*, Orlando, Florida, Apr. 8–12, 1996, pp. 86–97.
5. Pasquill, F., *Atmospheric Diffusion: The Dispersion of Windborne Material from Industrial and Other Sources*, 2nd ed., Wiley & Sons (Halstead Press), 1974.
6. Zrnich, Dusan S., "Estimation of Spectral Moments for Weather Echoes," *IEEE Transactions on Electronics*, vol. GE-7, no. 4, Oct. 1979, pp. 1248–1264.
7. Sonnenschein, C.M. and F.A. Horrigan, "Signal-To-Noise Relationships for Coaxial Systems That Heterodyne Backscatter from the Atmosphere," *Applied Optics*, vol. 10, no. 7, July 1971, pp. 2541–2546.
8. Houbolt, John C., Roy Steiner, and Kermit G. Pratt, *Dynamic Response of Airplanes to Atmospheric Turbulence Including Flight Data on Input and Response*, NASA TR R-199, June 1964.

REPORT DOCUMENTATION PAGE

Form Approved
OMB No. 0704-0188

Public reporting burden for this collection of information is estimated to average 1 hour per response, including the time for reviewing instructions, searching existing data sources, gathering and maintaining the data needed, and completing and reviewing the collection of information. Send comments regarding this burden estimate or any other aspect of this collection of information, including suggestions for reducing this burden, to Washington Headquarters Services, Directorate for Information Operations and Reports, 1215 Jefferson Davis Highway, Suite 1204, Arlington, VA 22202-4302, and to the Office of Management and Budget, Paperwork Reduction Project (0704-0188), Washington, DC 20503.

1. AGENCY USE ONLY (Leave blank)		2. REPORT DATE August 1996	3. REPORT TYPE AND DATES COVERED Technical Memorandum	
4. TITLE AND SUBTITLE Coherent Lidar Turbulence Measurement for Gust Load Alleviation			5. FUNDING NUMBERS WU 505-69-59	
6. AUTHOR(S) David Soreide, Rodney K. Bogue, L.J. Ehernberger, Hal Bagley				
7. PERFORMING ORGANIZATION NAME(S) AND ADDRESS(ES) NASA Dryden Flight Research Center P.O. Box 273 Edwards, California 93523-0273			8. PERFORMING ORGANIZATION REPORT NUMBER H-2117	
9. SPONSORING/MONITORING AGENCY NAME(S) AND ADDRESS(ES) National Aeronautics and Space Administration Washington, DC 20546-0001			10. SPONSORING/MONITORING AGENCY REPORT NUMBER NASA TM-104318	
11. SUPPLEMENTARY NOTES Presented as SPIE paper 2832-05 at the SPIE 1996 International Symposium on Optical Science, Engineering, and Instrumentation, August 4-9, 1996, Denver, Colorado. D. Soreide, Technical Consultant, Seattle, Washington. R.K. Bogue and L.J. Ehernberger, NASA Dryden Flight Research Center, Edwards, California. H. Bagley, Coherent Technologies, Inc., Boulder, Colorado				
12a. DISTRIBUTION/AVAILABILITY STATEMENT Unclassified—Unlimited Subject Category 06			12b. DISTRIBUTION CODE	
13. ABSTRACT (Maximum 200 words) Atmospheric turbulence adversely affects operation of commercial and military aircraft and is a design constraint. The airplane structure must be designed to survive the loads imposed by turbulence. Reducing these loads allows the airplane structure to be lighter, a substantial advantage for a commercial airplane. Gust alleviation systems based on accelerometers mounted in the airplane can reduce the maximum gust loads by a small fraction. These systems still represent an economic advantage. The ability to reduce the gust load increases tremendously if the turbulent gust can be measured before the airplane encounters it. A lidar system can make measurements of turbulent gusts ahead of the airplane, and the NASA Airborne Coherent Lidar for Advanced In-Flight Measurements (ACLAIM) program is developing such a lidar. The ACLAIM program is intended to develop a prototype lidar system for use in feasibility testing of gust load alleviation systems and other airborne lidar applications, to define applications of lidar with the potential for improving airplane performance, and to determine the feasibility and benefits of these applications. This paper gives an overview of the ACLAIM program, describes the lidar architecture for a gust alleviation system, and describes the prototype ACLAIM lidar system.				
14. SUBJECT TERMS Aircraft operation; Aircraft sensors; Backscatter; Gust; Lidar; Load alleviation; Turbulence			15. NUMBER OF PAGES 18	
			16. PRICE CODE AO3	
17. SECURITY CLASSIFICATION OF REPORT Unclassified	18. SECURITY CLASSIFICATION OF THIS PAGE Unclassified	19. SECURITY CLASSIFICATION OF ABSTRACT Unclassified	20. LIMITATION OF ABSTRACT Unlimited	